Discovery and Photometric Analysis of the δ Scuti Variable TYC 2168-132-1

Michael D. Joner
Eric G. Hintz
Department of Physics and Astronomy, Brigham Young University, N283 ESC, Provo, UT 84602; joner@byu.edu; hintz@byu.edu

Giorgio Corfini
Società Astronomica Lunae, Via Montefrancio, 77-1, Castelnuovo Magra, I-19030, Italy

Received August 23, 2016; revised November 7, 2016; accepted November 15, 2016

Abstract We detail the discovery of the short-period variable star presently known as TYC 2168-132-1. We have examined four nights of photometric observations of this star secured in 2015 and find it to be a δ Scuti variable with a primary period of 0.0737523 day. The star is multiperiodic with three dominant frequencies at 13.556, 7.047, and 11.757 cycles/day. Evidence from light curve morphology supports the δ Scuti classification. We estimate intrinsic values for color and luminosity that place TYC 2168-132-1 within the lower part of the instability strip.

1. Introduction

The Kilodegree Extremely Little Telescope (KELT) project (Pepper *et al.* 2007) is designed to find planetary transits of bright stars. During the KELT survey process, many variable objects are found and likely transit candidates are assigned an identifier and priority for follow-up observations. Of course, many variable objects are found in the survey that are not transit candidates. With the transit candidates, it is not uncommon for follow-up observers to find additional faint variable stars in the fields that are examined. These variable stars are generally found either during an examination of stars close to the KELT candidate in order to rule out a false positive from a blended source, or while selecting stars to serve as primary comparison sources within a field. In the case of TYC 2168-132-1, variation was detected during the observation of a KELT planetary transit candidate in survey Field 11 while selecting comparison stars. Giorgio Corfini (died December 2014) reported to the KELT Follow-Up Network (KFUN) on 7 August 2014 that he found variability in an object marked T10 on his finder image. He noted that he had checked the International Variable Star Index (VSX; Watson *et al.* 2014) maintained by the American Association of Variable Star Observers and did not find this star listed as a variable. Shortly after this report, it was realized that TYC 2168-132-1 had been noticed in the KELT survey but did not pass through the selection process for identification as a transit candidate. The newly reported depth estimate was promising enough that a decision was made to take another look at this target, which was then designated as KC11C050626 and assigned a rather low priority for follow-up observations.

There were two sets of data submitted for this target within a couple of days that clearly showed that the predicted planetary transit was unlikely. In one case, the observations were for a period of time that was shorter than the suspected transit window and the resulting light curve was reported as a saw tooth plot. In the other case, the shape of the light curve was such that the event was reported to be a deeper eclipse with a curious step just after the predicted egress. On UT 2014 August 16, the target was observed with the Brigham Young University West Mountain Observatory (WMO) 0.9-meter telescope for about four hours in the R filter. It was noted in the follow-up report to the KFUN that the resulting light curve appeared to be low amplitude pulsations from a multiperiodic δ Scuti variable star. These data are displayed in Figure 1.

After these observations the target was considered expired, but it remained on the candidate list at the lowest priority level until 21 September 2015 when the BVI data set given later in this paper was reported to the KFUN. The star was expired from the transit candidate list as the new BVI light curve varied amplitude with color, as would be expected from a δ Scuti variable star. At this point, it was absolutely certain that the observed variability was not due to a transit.

2. Observations

2.1. New observations

The new BVRI photometric data reported in this investigation were secured at WMO with the 0.9-meter telescope. The detector used for these observations is a Fairchild 3041-UV CCD mounted in a FLI ProLine camera. The CCD is a 2048 × 2048 array with 15-micron pixels. The plate scale

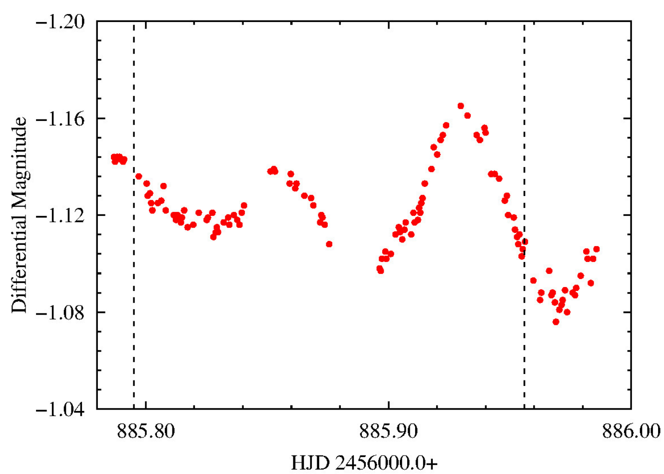

Figure 1. Light curve for TCY 2168-132-1 on UT 2014 August 16 that clearly showed that the observed variability was not due to a suspected planetary transit. The predicted times of ingress and egress for the previously suspected transit are shown as vertical dashed lines.

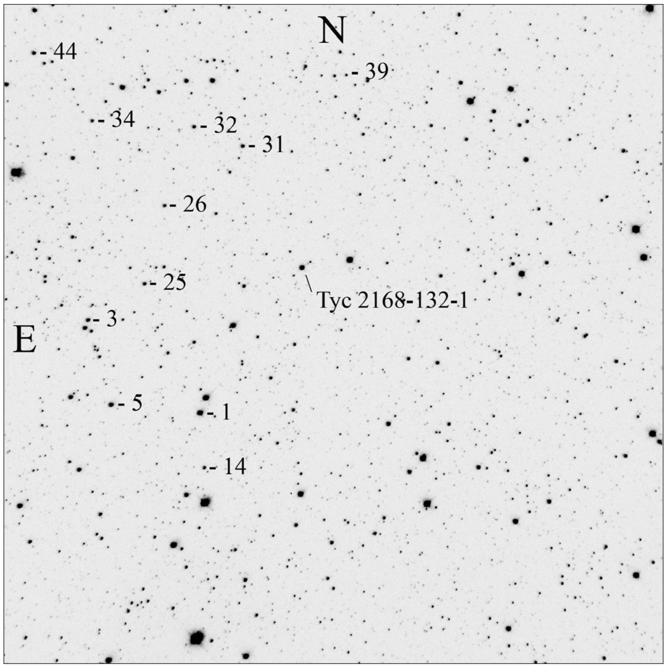

Figure 2. Finder chart for TYC 2168-132-1 from the 0.9-meter telescope at WMO. The field of view is a square 20.5'. Comparison stars and suspected longer period variable stars are marked as described in the text.

at the f/5.5 Cassegrain focus is 0.61"/pixel. During final processing, the frames are trimmed to 2000 × 2000 pixels, giving a square field of view that is 20.5' on a side. Standard BVRI Johnson/Cousins filters from Astrodon Photometrics were used for all observations. Each of the raw images was processed using standard IRAF routines to make overscan, trim, zero, dark, and flat field corrections before doing any analysis of the image data.

The WMO time series data for TYC 2168-132-1 was first obtained in the R filter on UT 2014 August 16. Four additional nights of observations were made between 2015 September 21 and October 14 in B, V, R, and I filters. A frame of the field examined is shown in Figure 2 with the primary target, a number of suspected variable stars with longer periods, comparison stars, and check stars marked. This field is 20.5' square and was taken using a standard V filter. Photometric values were determined using comparison stars 1, 3, 14, 26, 31, and 32. Along with these comparison stars, we also used stars 5 and 25 as check stars. In addition to the variations seen in our target star, we found that stars 34, 39, and 44 showed longer term variability of 0.05 magnitude or greater and are possibly eclipsing binaries with periods of several days to a week or more.

All the check and comparison stars had errors per observation of 0.011 or less in the combined four-night solution in V. A few of the reference stars had values listed in APASS (Henden *et al.* 2015), and these stars were used to establish a zero point for the B and V differential light curves. Multiple solutions were done in VPHOT using the comparison and check star sample given above. An iterative approach was used to improve the magnitude values in each filter for each star until the solutions converged to the final values used in the analysis.

2.2. Archive data

A search of the NASA/IPAC archive shows data for TYC

Table 1. Archive photometric measurements of TYC 2168-132-1. Magnitudes and Fν.

Filter	*TYC 2168-132-1 mag.*	*TYC 2168-132-1 mJy.*
B	12.418 ± 0.027	46.0
V	11.921 ± 0.019	65.4
J	10.760 ± 0.019	79.2
H	10.520 ± 0.020	63.4
K	10.432 ± 0.016	44.8
W1	10.366 ± 0.023	21.6
W2	10.389 ± 0.020	12.0
W3	10.470 ± 0.100	2.1
W4	9.130 ± 0.463	1.9

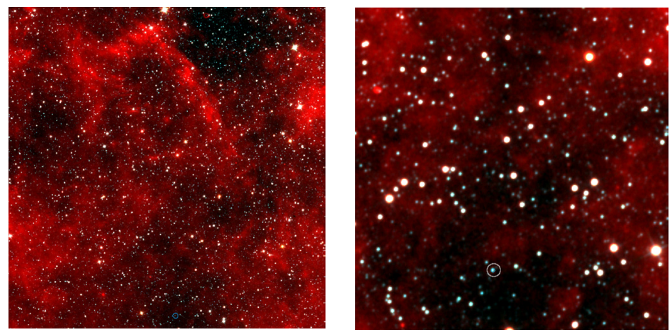

Figure 3. WISE Multi-Color Image from all four filters. The left image shows the full field which includes TYC 1268-132-1. A circle near the bottom of the frame marks the target. The right image is a 20' region zoomed in around the target.

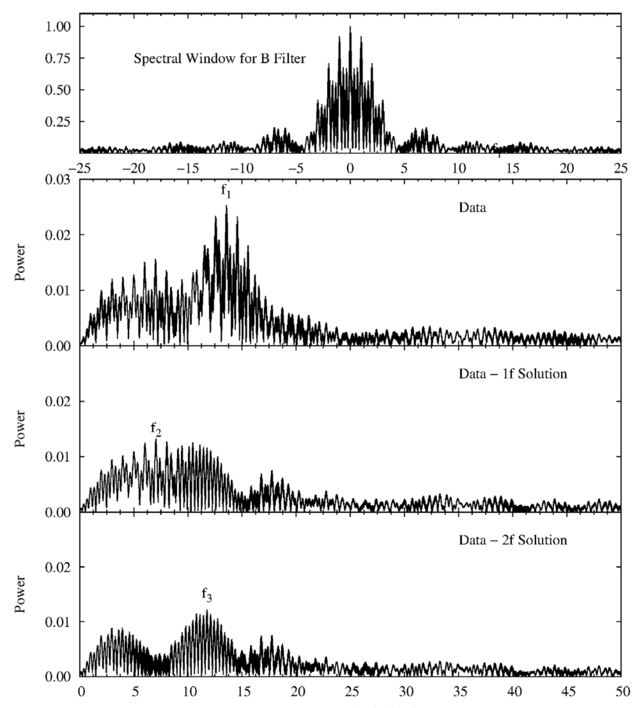

Figure 4. The power spectrum from the B filter for the first three frequencies.

2168-132-1 from the 2MASS Point Source Catalog (Skrutskie *et al.* 2006) and a number of listings from the WISE satellite mission (Wright *et al.* 2010; Mainzer *et al.* 2011). We have collected the measured magnitudes and examined a number of the published images from these sources to supplement the data used in this analysis. In Table 1 we display the average magnitude and flux for each filter. In addition, we collected individual measurements from the WISE W1 and W2 filters from the WISE All-Sky Single Exposure Source Table, the WISE Post-Cryo Single Exposure Source Table, and the NEOWISE-R Single Exposure Source Table. We were also able to examine a number of individual frames from the WISE AllWISE Release Atlas Image. This included the multicolor image shown in Figure 3 with the target marked with a circle near the bottom of the field. The field on the right is 20' on a side so that it matches the dimensions from Figure 2.

The WISE data came in four distinct observing groups; May 2010, November 2010, May 2014, and November 2014. Each group consisted of 16 or 17 observations taken over about a 1.25-day time frame, with an image secured about every two hours. This provided a total of 63 observations in the W1 and W2 filters. Clearly, these data would not be useful in the determination of times of maximum light given that the cadence is similar to the pulsation period as discussed later.

3. Analysis

3.1. Fourier decomposition

To begin our analysis, we examined the four nights of new data obtained in 2015 using PERIOD04 (Lenz and Breger 2005) to find the detectable pulsation frequencies in our target. The analysis proceeded for each of the four filters: B, V, R, and I. The B, V, and I observations are included in all four nights of new data, while the R observations were made on only the last three of those nights. For the B, V, and I nights the initial three frequencies were consistently 13.556 ± 0.001, 7.047 ± 0.002, and 11.757 ± 0.002 cycles / day. The primary frequency corresponds to a period of 0.07376 ± 0.00001 day. In Figure 4 and Figure 5 we show the spectral window and power spectrum for the first three frequencies in the B and V filters, respectively. It is interesting to note that the second and third frequencies reverse order between the two filters. For each filter we found additional frequencies that would be considered within the detection limit of Breger *et al.* (1993). However, given the lack of consistency across the four filters we have chosen to only report the first three frequencies that repeat across all four filters. The amplitudes for each frequency are gathered in Table 2, along with the S/N level for each.

We have a high level of confidence in the primary frequency detailed above. It is in excellent agreement with period determined from a times of maximum light analysis detailed below. An examination of the power spectra for the second and third frequencies doesn't make as strong a case; however, we feel that the consistency across filters argues strongly for these two additional frequencies. It is of note that the amplitude at each frequency decreases as we go from the B filter to the I filter, as would be expected for a pulsating variable such as a δ Scuti star. The data for all four nights of multi-filter photometry,

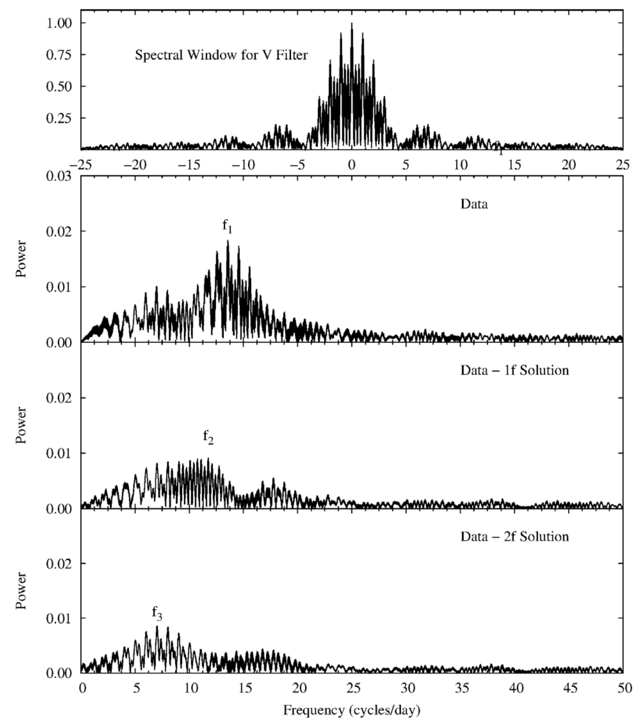

Figure 5. The power spectrum from the V filter for the first three frequencies.

Table 2. Fourier frequencies by filter.

Frequency	*B Ampl.*	*B S/N*	*V Ampl.*	*V S/N*	*R Ampl.*	*R S/N*	*I Ampl.*	*I S/N*
13.556 ± 0.001	0.025	15.8	0.019	20.7	0.012	13.2	0.011	11.9
7.047 ± 0.002	0.016	6.5	0.009	8.9	0.006	17.3	0.004	2.4
11.757 ± 0.002	0.013	8.6	0.008	10.3	0.008	9.9	0.005	4.4

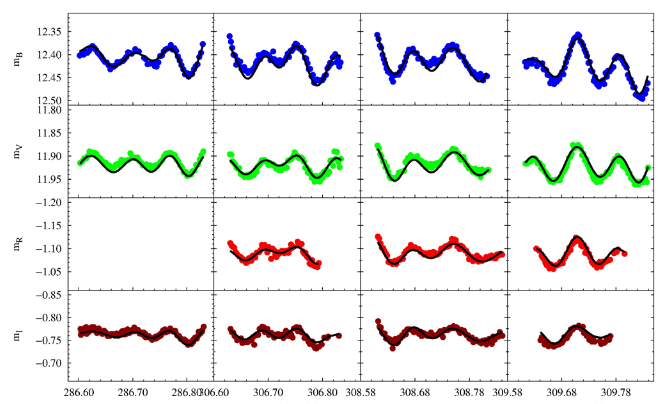

Figure 6. Four nights of multi-filter photometry along with the best Fourier fit for each filter.

along with the best Fourier fit for each filter from the frequency analysis described above, are displayed in Figure 6. We note that the two additional frequencies improve the curve that is fit to the observed data in the light curves displayed for each filter in Figure 6.

Using the Fourier fits to the B and V data, we determined a B–V curve for TYC 2168-132-1. In the upper panel of Figure 7 we show the B data and the Fourier fit to the B data for the four nights from 2015. In the lower panel of the figure we show the B–V curve from the two Fourier fits. The frequencies found,

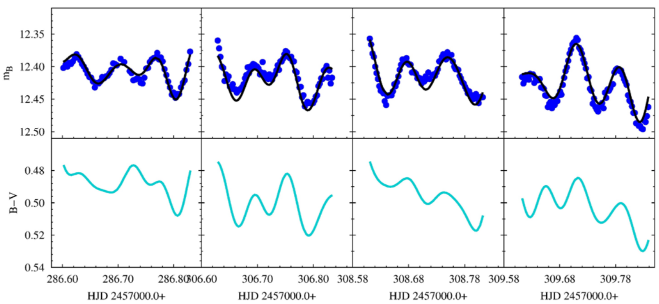

Figure 7. B–V curves from Fourier fits for TYC 2168-132-1 compared to the B-filter observations.

Table 3. Times of maximun light 2450000.0+.

Cycle Number	*B Time*	*V Time*	*R Time*	*I Time*
–5434	—	—	6885.85275	—
–5433	—	—	6885.93004	—
0	7286.62607	7286.62533	—	7286.62381
1	7286.70416	7286.70052	—	7286.69546
2	7286.76948	7286.76823	—	7286.76726
272	7306.69315	7306.69308	7306.69394	7306.69095
273	7306.75302	7306.75070	7306.75494	7306.75332
299	7308.67316	7308.67306	7308.67425	7308.67000
300	7308.74799	7308.74879	7308.75103	7308.75053
313	7309.70924	7309.70818	7309.70857	7309.70873
314	7309.78528	7309.78345	—	—

and the shape of the B–V curve, lead us to the conclusion that this star is a pulsating variable of the δ Scuti type.

Finally, we examined the data from the WISE satellite for TYC 2168-132-1. The reported error per observation for the various WISE data sets is on the order of 0.02 magnitude, which makes it unlikely that we would see the variations in such a low amplitude variable star. However, we gathered the data from the WISE All-sky Single Exposure Source Table and the NEOWISE-R Single Exposure data tables. The data from the Post-Cryo series were found to have larger errors and were not included in this analysis. In the WISE database the times of observation were given as Modified Julian Days (MJD). To match our other observations we converted those MJD values to Heliocentric Julian Days (HJD). Again, we used PERIOD04 to examine the WISE data. Given the poor spectral window from the sparse data we used the frequency at 13.556 cycles / day to phase the data and estimate the amplitude. For both the W1 and W2 filters the error on the amplitude is comparable to the amplitude, but is clearly less than 0.01.

This is reasonable when compared with the decreasing amplitudes with wavelength we reported earlier for the BVRI filters.

3.2. Times of maximum light

The next stage of our analysis was to examine the times of maximum light. To do this we used the PERANSO software (Paunzen and Vanmunster 2016) in order to apply two different methods to each maximum in our data set. We first used the Kwee and van Woerden (1956) method within PERANSO. We then applied a polynomial fit to each maximum to get a second estimate of each time of maximum light. For the B and V filters we found nine times of maximum light from the four nights of data. For the I filter we found eight times of maximum light, missing the last time on the last night. The determination of times of maximum light was most difficult for the R filter, where we have five times of maximum light that correspond to the nights that were also observed in B, V, and I. In addition, there are two additional times of maximum light from the 2014 R light curve. We report these times of maximum light in Table 3, where the reported time is the average of the two methods discussed above. In most cases, both methods provided reasonable estimates of the time of maximum light with only small differences.

To provide the longest range in time, we averaged the observed times of maximum light over the four filters. Using the period determined from the Fourier fits, we determined the cycle number of each observation. Fitting a linear regression to this set of data, we find an ephemeris as given in Equation 1.

$$\mathrm{HJD} = 2457286.6242(9) + 0.0737523(4)E \qquad (1)$$

Using this ephemeris, we determined O–C values for each average time of maximum light. The resulting values scatter evenly about a zero line. The period determined here closely matches the period associated with the f1 value from the Fourier fits. The O–C curve is shown in Figure 8. With such a short baseline, it is not surprising that the resulting curve is flat. We also note that there is a fairly wide range in values of O–C for a given epoch. We believe this is expected for a strongly modulated light curve in a multiperiodic star like TYC 2168-132-1.

3.3. Reddening and B–V color

As detailed in the observing section, our B filter and V filter observations were calibrated with nearby comparison stars. We measure B–V for the variable star in the range of 0.48 to 0.53. Even though it is slightly beyond the red edge of the instability strip, that range is reasonable to expect for a lightly reddened δ Scuti star in the instability strip close to the main sequence. Furthermore, from the image shown in Figure 3 it is clear from the visible material that our target could be significantly reddened. This is not surprising given the galactic coordinates for longitude and latitude of TYC 2168-132-1 of 68.772° and −5.13°, respectively. Using the maps of Schlafly and Finkbeiner (2011) we find an E(B–V) of 0.645 in the direction of our target. This reddening would be the maximum reddening that our star could experience. The actual reddening for a nearby star would likely be significantly less, but this upper limit is clearly sufficient to show the plausibility of the values estimated in the next section.

Given that δ Scuti variables normally lie in the spectral type range from about A5 to F5, we can estimate an approximate reddening range for our target. To keep the star within the instability strip, the E(B–V) needs to be in the range of 0.08 to 0.32. Using these E(B–V) values, we determined absorption values for each of our filters based on the methods detailed in Schlafly and Finkbeiner (2011). Using these values, we deredden our data and the archival data to generate SEDs for our object, which are shown in Figure 9. The lowest curve in Figure 9 is the observed curve with no reddening correction

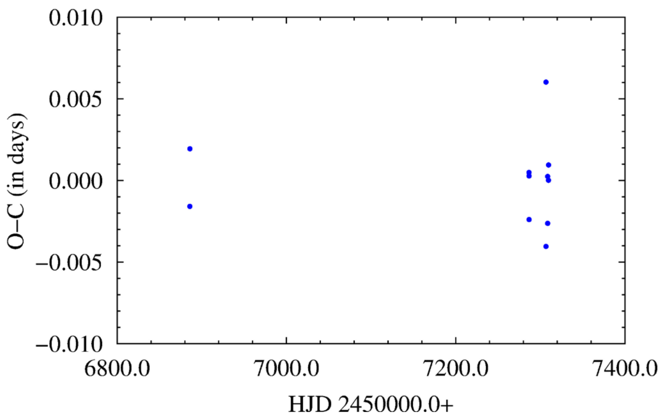

Figure 8. O–C diagram for TYC 2168-132-1.

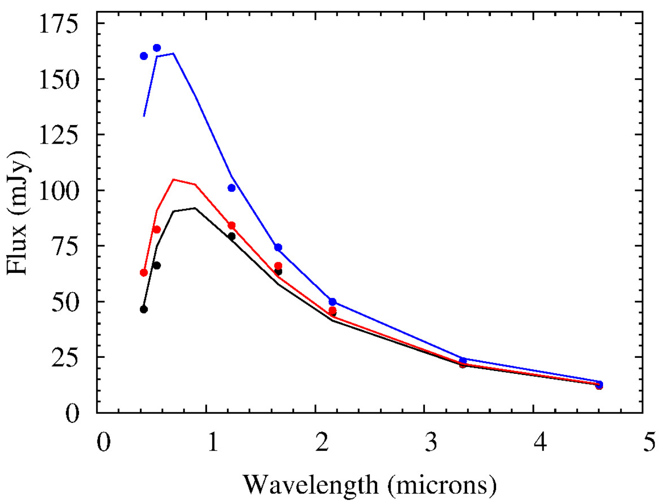

Figure 9. The spectral energy distribution plots for TYC 2168-132-1. Observed curve shown in black (bottom), the curve with a reddening correction for the red edge of instability strip shown in red (middle), and the curve with a reddening adjustment for the blue edge of the instability strip shown in blue (top).

applied. The middle curve was generated using values from Schlafly and Finkbeiner (2011) for E(B–V) = 0.08, for a star at the red edge of the instability strip. Finally, the top curve in Figure 9 is the curve based on values for E(B–V) = 0.32, corresponding to a star at the blue edge of the instability strip. Starting with the (B–V) for each curve, we used the relations in Flower (1996) and Torres (2010) to estimate the temperature for each SED. We then used a scaled Planck function to fit a blackbody curve to each data set. The blackbody fits are overlaid on the corresponding SED in Figure 9.

The scale factor used to bring the observed values in line with blackbody values is 5.7×10^{-21}. The square root of this value is the ratio of the radius of the target to the distance to the target. Therefore, we find a value of $r/R = 7.5 \times 10^{-11}$. Since the previous evidence presented in this paper points to this object being a δ Scuti variable, we can estimate the radius of our object. Given a target inside the instability strip, in the luminosity class range of IV–V, we calculate a radius of about 2.3 $R_{\odot}$. This estimate leads to a distance of approximately 700 parsecs.

4. Conclusion

We have summarized the discovery of variability for the former KELT target star TYC 2168-132-1. We present and analyze new data for the recently discovered variable star. Analysis of the data is done and provides evidence in support of the δ Scuti hypothesis. We show that the observed variations can be fit using Fourier decomposition techniques. The star is found to be periodic with three dominant frequencies at 13.556, 7.047, and 11.757 cycles / day. The results are similar to other pulsating variables in the δ Scuti class with the new data showing a primary period of 0.0737523 day. Evidence from light curve morphology also supports the suggested δ Scuti classification. We estimate intrinsic values for color and luminosity that place TYC 2168-132-1 within the lower region of the instability strip. With an estimated radius of 2.3 $R_{\odot}$ we find a distance of about 700 parsecs.

5. Acknowledgements

We thank Joao Gregorio and Eric L. N. Jensen for initial observations of KC11C050626 in the KELT Follow-up Network that helped first confirm the variable nature of this star. We thank all the KELT team members for their efforts in organizing and managing a project of this complexity. We also thank Roberto Zambelli and Josh Pepper for comments and direction given during the early stages of writing this paper. We acknowledge the Brigham Young University Department of Physics and Astronomy for its continued support of our research efforts. This research has made use of the APASS database, located at the AAVSO web site. Funding for APASS has been provided by the Robert Martin Ayers Sciences Fund. This publication makes use of data products from the Wide-field Infrared Survey Explorer, which is a joint project of the University of California, Los Angeles, and the Jet Propulsion Laboratory/California Institute of Technology, funded by the National Aeronautics and Space Administration. This publication also makes use of data products from NEOWISE, which is a project of the Jet Propulsion Laboratory / California Institute of Technology, funded by the Planetary Science Division of the National Aeronautics and Space Administration. This publication makes use of data products from the Two Micron All Sky Survey, which is a joint project of the University of Massachusetts and the Infrared Processing and Analysis Center / California Institute of Technology, funded by the National Aeronautics and Space Administration and the National Science Foundation.

Facility: BYU:0.9m, WISE, FLWO:2MASS, AAVSO
Software: IRAF, VPHOT, ASTROIMAGEJ

References

Breger, M., *et al.* 1993, *Astron. Astrophys.*, **271**, 482.
Flower, P. J. 1996, *Astrophys. J.*, **469**, 355.
Henden, A. A., *et al.* 2015, AAVSO Photometric All-Sky Survey, data release 9 (http://www.aavso.org/apass).
Kwee, K., and van Woerden, H. 1956, *Bull. Astron. Inst. Netherlands*, **12**, 327.
Lenz, P., and Breger, M. 2005, *Commun. Asteroseismology*, **146**, 53.
Mainzer, A., *et al.* 2011, *Astrophys. J.*, **731**, 53.

Paunzen, E., and Vanmunster, T. 2016, *Astron. Nachr.*, **337**, 239.
Pepper, J., *et al.* 2007, *Publ. Astron. Soc. Pacific*, **119**, 923.
Schlafly, E. F., and Finkbeiner, D. P. 2011, *Astrophys. J.*, **737**, 103.
Skrutskie, M. F., *et al.* 2006, *Astron. J.*, **131**, 1163.
Torres, G. 2010, *Astron. J.*, **140**, 1158,
Watson, C., Henden, A. A., and Price, C. A. 2014, AAVSO International Variable Star Index VSX (Watson+, 2006–2014; http://www.aavso.org/vsx).
Wright, E. L., *et al.* 2010, *Astron. J.*, **140**, 1868.